Journal of Hydrology 368 (2009) 262–275

Contents lists available at ScienceDirect

Journal of Hydrology

journal homepage: www.elsevier.com/locate/jhydrol

Flood routing and alluvial aquifer recharge along the ephemeral arid Kuiseb River, Namibia

Efrat Morin [a,*], Tamir Grodek [a], Ofer Dahan [b], Gerardo Benito [c], Christoph Kulls [d], Yael Jacoby [a], Guido Van Langenhove [e], Mary Seely [f], Yehouda Enzel [g]

[a] Department of Geography, The Hebrew University of Jerusalem, Mt. Scopus, Jerusalem 91905, Israel
[b] Zuckerberg Institute for Water Research, Ben-Gurion University of the Negev, Sde Boqer 84990, Israel
[c] Centro de Ciencias Medioambientales, Consejo Superior de Investigaciones Científicas, Serrano 115 Bis, 28006 Madrid, Spain
[d] Institute of Hydrology, University of Freiburg, Freiburg 79098, Germany
[e] Ministry of Agriculture, Water and Forestry, Department of Water Affairs and Forestry, Hydrology Division, Windhoek, Namibia
[f] Desert Research Foundation of Namibia, 7 Rossini St., Windhoek, Namibia
[g] Institute of Earth Sciences, The Hebrew University of Jerusalem, Givat Ram, Jerusalem 91904, Israel

ARTICLE INFO

Article history:
Received 20 March 2008
Received in revised form 15 September 2008
Accepted 7 February 2009

This manuscript was handled by K. Georgakakos, Editor-in-Chief, with the assistance of Ehab A. Meselhe, Associate Editor

Keywords:
Alluvial shallow aquifer
Aquifer recharge
Arid zone
Flash flood infiltration
Transmission loss
Africa

SUMMARY

Flood water infiltrates ephemeral channels, recharging local and regional aquifers, and it is the main water source in hyperarid regions. Quantitative estimations of these resources are limited by the scarcity of data from such regions. The floods of the Kuiseb River in the Namib Desert have been monitored for 46 years, providing a unique data set of flow hydrographs from one of the world's hyperarid regions. The study objectives were to: (1) subject the records to quality control; (2) model flood routing and transmission losses; and (3) study the relationships between flood characteristics, river characteristics and recharge into the aquifers. After rigorous quality-testing of the original gauge-station data, a flood-routing model based on kinematic flow with components accounting for channel-bed infiltration was constructed and applied to the data. A simplified module added to this routing model estimates aquifer recharge from the infiltrating flood water. Most of the model parameters were obtained from field surveys and GIS analyses. Two of the model parameters—Manning's roughness coefficient and the constant infiltration rate—were calibrated based on the high-quality measured flow data set, providing values of 0.025 and 8.5 mm/h, respectively. This infiltration rate is in agreement with that estimated from extensive direct TDR-based moisture measurements in the vadose zone under the Kuiseb River channel, and is low relative to those reported for other sites. The model was later verified with additional flood data and observed groundwater levels in boreholes. Sensitivity analysis showed the important role of large and medium floods in aquifer recharge. To generalize from the studied river to other streams with diverse conditions, we demonstrate that with increasing in infiltration rate, channel length or active channel width, the relative contribution of high-magnitude floods to recharge also increases, whereas medium and small floods contribute less, often not reaching the downstream parts of the arid ephemeral river at all. For example, more than three-quarters of the floods reaching the downstream Kuiseb River (with an infiltration rate of 8.5 mm/h) would not have reached similar distances in rivers with all other properties similar but with infiltration rates of 50 mm/h. The recharge volume in the downstream segment in the case of higher infiltration is mainly contributed by floods with magnitude $\geqslant$93rd percentile, compared to floods in the 63rd percentile at an infiltration rate of 8.5 mm/h.

Introduction

Floods are the main source of water in most of the world's arid lands. Transmission losses, where flood water infiltrates the ephemeral channel-bed, supply the necessary moisture for vegetation, and recharge alluvial aquifers. Although flow in arid channels is rare and the water volumes are relatively small, the infiltrated flood water provides the water resources necessary for maintaining human settlements, riparian vegetation and wildlife along the rivers. In addition, the transmission losses control flood hydrology in arid, and even more so in hyperarid environments. Therefore, an understanding of floods and their associated transmission losses and recharge into alluvial aquifers is crucial for understanding water resources.

* Corresponding author. Tel.: +972 2 5883020; fax: +972 2 5820549.
E-mail address: msmorin@mscc.huji.ac.il (E. Morin).

0022-1694/$ - see front matter © 2009 Elsevier B.V. All rights reserved.
doi:10.1016/j.jhydrol.2009.02.015

Previous efforts to quantify water losses and study flood routing in ephemeral arid rivers (Freyberg et al., 1980; Guzman et al., 1989; Walters, 1990; Hughes and Sami, 1992; Knighton and Nanson, 1994; Sharma and Murthy, 1994; Sorman et al., 1997; El-Hames and Richards, 1998; Shentsis et al., 1999; Izbicki et al., 2002; Costelloe et al., 2003; Blasch et al., 2004, 2006) have produced limited results due to: (a) scarce gauge record availability in arid and hyperarid channels, particularly with more than one gauge station; (b) a small number of flow events, including years with no floods at all; (c) too little applicative interest—most of the time these channels support only small communities, and (d) logistical difficulties—such rivers are usually in remote parts of hyperarid environments (Schick, 1988). Typical humid drainage-basin discharge increases downstream; however, in dry environments, peak discharge and flood volumes are often reduced downstream when flowing over ephemeral alluvial channels (Schick, 1988). Tooth (2000), summarizing studies of transmission losses in arid rivers of Australia, India, Saudi Arabia and Arizona, reported a downstream reduction of between 8% and 95% of flood volumes and peak discharges (Renard and Keppel, 1966; Walters, 1990; Knighton and Nanson, 1994). The controlling factors of flood hydrographs and transmission losses in these areas include peak discharge (Enzel, 1992), flood frequency, hydrograph shape and type (Knighton and Nanson, 1994), river length (Dubief, 1953; Vanney, 1960; Buono and Lang, 1980; Knighton and Nanson, 1994; Thornes, 1994; Enzel and Wells, 1997), and texture of the channel-bed sediment.

Transmission-loss research on large systems (10^4–10^5 km^2) is even less common (Knighton and Nanson, 1994). A few classic studies describe the Guir-Saoura-Messaoud system which begins in the higher and wetter Atlas Mountains and flows a distance of ~1000 km through the Sahara Desert into which most of the flood water infiltrates, less than 10% reaching the lower river section (>700 km downstream) (Dubief, 1953; Vanney, 1960; Mabbutt, 1977). A typical configuration of these large ephemeral river systems includes a catchment headwater located under sub-humid or semiarid rainfall conditions which generates floods, reaching a lower catchment area located under arid or hyperarid conditions which feeds alluvial aquifers. This is also the case for the Kuiseb River (central-western Namibia, Fig. 1a), whose relatively wetter headwaters (>300 mm) are able to generate floods almost every year that overcome the transmission losses along its long course and reach various distances along the middle-lower hyperarid reaches crossing the Namib Desert (Mendelsohn et al., 2002). In the middle-lower Kuiseb (lower 100 km), the river develops an extensive sandy, braided alluvial channel and floodplain (Theron et al., 1980) connected to shallow aquifers which are recharged by infiltrated flood waters and are the main source of water for human life, flora and fauna in the desert environment.

In this paper, we highlight the potential of flood routing and transmission-loss methods, when appropriate data are available, and discuss the parameters controlling recharge in the lower reaches of the Kuiseb River (Namib Desert). The main objectives are to: (1) analyze the quality of the gauge-station data, and eliminate possible errors by cross-checking the data series from different stations; (2) develop new tools for modeling flood routing and transmission losses accounting for the main factors affecting these processes; and (3) study the relationships between flood characteristics (e.g., peak, volume, duration), river characteristics (e.g., channel width, floodplain size) and recharge into the alluvial aquifers.

The Kuiseb River

The Kuiseb River (22°30′–23°45′S 14°30′–17°00′E) (Fig. 1a) in western Namibia drains an area of 15,500 km and is one of the

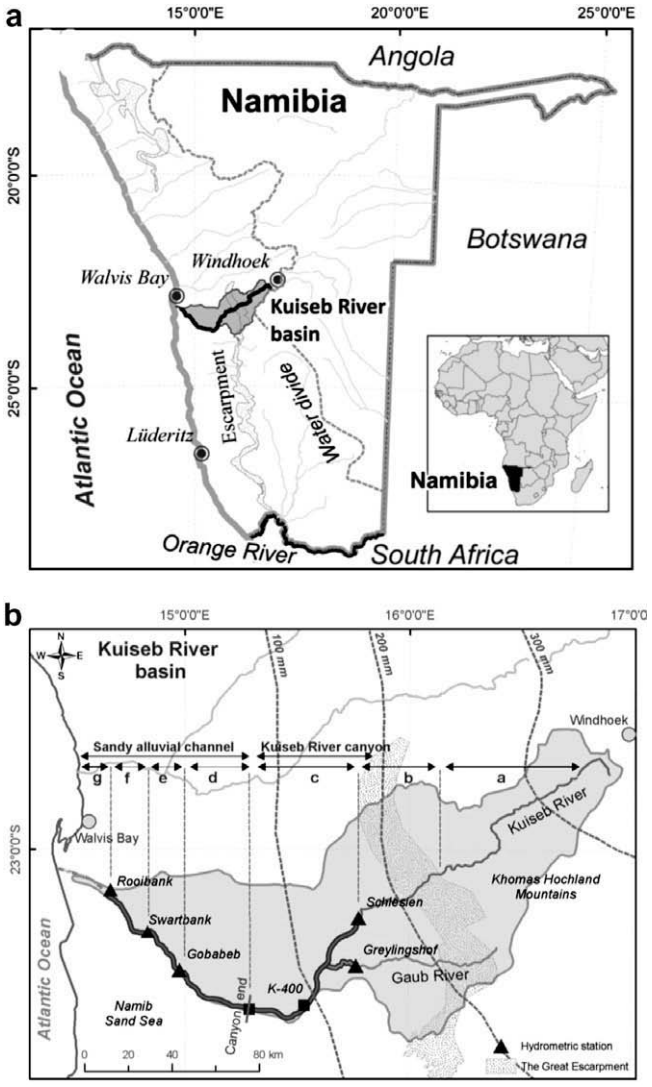

Fig. 1. (a) The general location of Namibia within the African continent and the study area within Namibia and (b) study area with annual rainfall contours, hydrometric stations (triangles), and river segments (Table 1).

12 major ephemeral rivers that flow from Namibia's main elevated water divide westward, cutting through or heading at the Great Escarpment and flowing across western Namibia towards the Atlantic Ocean (Jacobson et al., 1995).

The precipitation over the Kuiseb River basin (Jacobson et al., 1995; Mendelsohn et al., 2002) is characterized mainly by summer rains that alter sharply from a mean 350 mm/year at its headwaters at 2000 m above sea level (masl) to ~10 mm/year near Walvis Bay (Fig. 1b). As dictated by the spatial distribution of the rainfall, the river floods originate in the wetter upstream sections over the escarpment and the plateau east of it, while the lower reaches contribute insignificant, if any flow at all (Jacobson et al., 1995).

The following river segment description (see also Fig. 1b and Table 1) is based on maps and Geographical Information System (GIS) analysis and on field observations from three seasons of expeditions along the lower segments of the Kuiseb River (Fig. 1b segments c–g):

Segment a

From the headwater to the Great Escarpment—the mountainous headwaters begin in the Khomas Hochland mountains at

Table 1
River and model segments.

River segment (Fig. 1b)	Characteristics	Annual rainfall (mm/year) (interp.)	Model segment (Fig. 5a)	Length (km)	Slope	Active channel width (m)	Height to floodplains (m)	Floodplain width (m)	Aquifer width (m)	Recession rate (m/year)
a	Mountainous	250–350	–	120	0.0060	–	–	–	–	–
b	Escarpment	150–250	–	50	0.0350	–	–	–	–	–
c	Bedrock canyon	100–150	c1	40	0.0034	51	–	–	–	–
			c2	21	0.0034	40	–	–	–	–
			c3	33	0.0018	36	–	–	–	–
		50–100	c4	28	0.0018	33	–	–	–	–
d	Alluvial channel and relatively wide floodplains	25–50	d	55	0.0009	50	1.2	282	100	1.8
e		20–25	e	30	0.0009	68	1.2	567	500	0.5
f		10–20	f	33	0.0009	74	1.2	1027	1500	0.3
g		10	–	–	–	–	–	–	–	–

~2000 masl. The drainage lines follow joints and dissect this area into gently sloping hills covered by thin stony soil that supports an open savanna of low trees and shrubs. The relatively high summer rains (250–350 mm/year) in this segment are the main source for the downstream river floods.

Segment b

In this escarpment segment, the elevation drops dramatically, by approximately 1000 m, to the Namib Desert. The vegetation changes to more arid-type plants due to the shallow soils and lower annual rainfall (150–250 mm/year). The steep slopes form a relatively dense drainage network.

Segment c

At the foothill of the Great Escarpment, the river incises the schist bedrock to form the up to 200 m deep and ~35 m wide Kuiseb River Canyon. The Gaub River joins the Kuiseb River in the canyon and has a canyon of its own. The channel slope is ~0.3% for 150 km till the end of the canyon. The rainfall decreases from ~150 to 0 mm/year from the upper to the lower ends of canyon. Only very short first-order channels drain directly into the canyon. In between the mostly exposed bedrock sections in the canyon channel-bed, alternating sections of sand and gravel alluvium can be found. This alluvium is usually saturated to the level of wet quicksand and the wildlife benefits from water pools throughout the dry austral winter. This observation suggests very limited water loss along the canyon section.

Segment d

From the end of the Kuiseb River Canyon to the Gobabeb hydrometric station—the channel morphology changes dramatically from bedrock canyon to sandy braided alluvial channel with accretionary sandy islands that form floodplains in places. The slope decreases to less than 0.1% and the channel develops a 250- to 300-m wide floodplain with a characteristic width of ~280 m; the active channel remains relatively narrow, about 50 m, for the next 55 km. The alluvium becomes deep enough to establish a local shallow aquifer along the river course. In general, the length of the sandy river bed is divided into several compartments separated by high near-surface and exposed bedrock. This structure blocks the continuation of the relatively fast groundwater flow along the channel. The sediment grain size is >94% sand (63 and 560 μm) with ~6% silt and clay. During low to medium floods, the channel maintains its course and relatively dense vegetation, including well-grown trees, is established on the floodplains enjoying the relatively high water table (Seely et al., 1981; Fig. 2). Rare high-magnitude floods may shift the river course, create new floodplains or erode or laterally accrete existing ones, and new vegetation is established. Point TDR-based measurements of infiltrated water fluxes and groundwater level conducted in this segment by Dahan et al. (2008) indicate a relatively constant infiltration rate in the range of 7–10 mm/h independent of flood magnitude or flow duration. In response to the infiltrated water fluxes, groundwater level rises. In rare cases of long-duration floods, the groundwater level reaches the surface and transmission losses and recharge cease. Between the flood events, which can be months apart, groundwater level falls, initially at a relatively fast

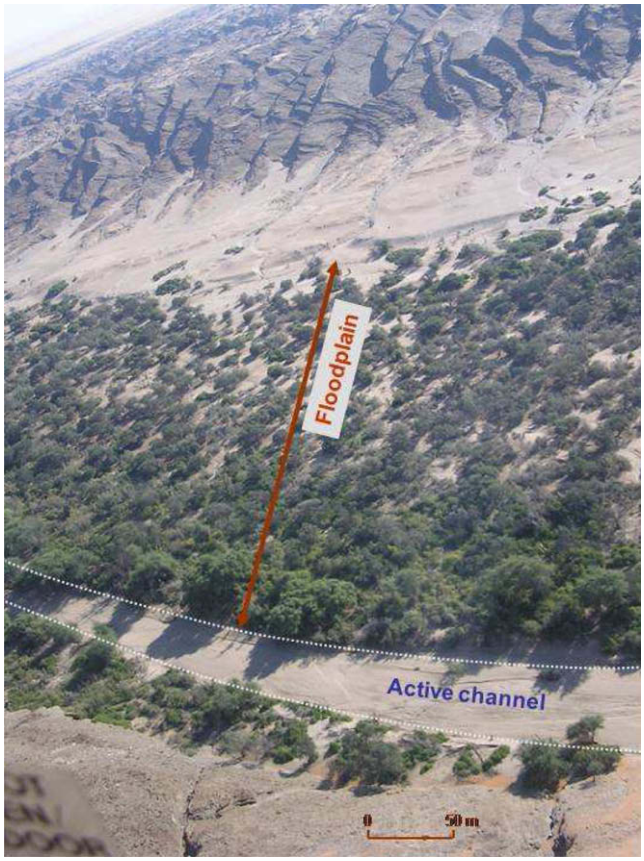

Fig. 2. A typical cross-section of segment d (see 'The Kuiseb River'). A sandy braided alluvial channel with an active channel of about 50 m and typically 250- to 300-m wide floodplains. The relatively dense vegetation over the floodplains is maintained by the high water table recharged by the river floods. Vegetation density decreases with distance from the active channel due to increasing distance to the groundwater and higher salinity. The elevated abandoned terraces at the base of the mountain front are high enough above the local aquifer to prevent the growth of vegetation.

rate, probably because the water flows laterally from underneath the channel to fill the entire width of the aquifer between its bedrock boundaries. Thereafter, the water table falls at the slower rate of ~5 mm/day. This decay is primarily dominated by evapotranspiration (Bate and Walker, 1993) of the dense riparian vegetation (Fig. 2) and by the longitudinal-compartment structure of the aquifer.

Segment e

This segment is 30 km long, between the Gobabeb and the Swartbank hydrometric stations. On average the channel width is about 560 m and the active width is limited to about 70 m. The potential water storage of the aquifer in this segment greatly increases because of the thick alluvial fill.

Segment f

This segment is between Swartbank and Rooibank hydrometric stations with an average channel width of ~1000 m, an active width of ~75 m and a deep alluvium. Several pumping fields in this segment extract water at a rate of about 6×10 m^3/year.

Segment g

This segment is ~25 km long, from Rooibank to the Atlantic Ocean near Walvis Bay. The channel meanders through coastal sand dunes in the south and through the port city of Walvis Bay. Near the coast, the river widens over a bed of unconsolidated sands. Floods have been recorded as reaching this section only 16 times since 1837.

Hydrological records

The flow data in several locations along the Kuiseb River and at its main tributary, the Gaub River, are monitored by the Ministry of Agriculture, Water and Forestry, Department of Water Affairs, Hydrology Division, Windhoek, and Namibia. Three hydrometric stations with sufficient data quality operate in the Kuiseb River basin below the Great Escarpment (Fig. 1b, the Schlesien, Greylingshof, and Gobabeb stations). Two additional hydrometric stations at the lowermost sections of the river (the Swartbank and Rooibank stations) unfortunately did not supply data with adequate quality for this study. Continuous measurement of flood data along the Kuiseb River basin started in 1960 with the Schlesien hydrometric station. Two additional hydrometric stations were installed in 1974 (the Greylingshof station in the Gaub River) and 1977 (the Gobabeb station).

Typical of remote areas, the quality of the Kuiseb River data is often questionable and therefore, we examined them closely to ensure that they were of adequate quality before using them in any further hydrological analyses. The availability of data from multiple stations allowed us to identify errors by cross-checking the hydrographs at the different stations. An example of a problem found in the flood data of the Gobabeb station is presented in Fig. 3. The hydrograph remains at a constant high discharge level rather than showing the typical desert recession to near zero. Our experience with desert stations in general, and with this station in particular, suggests that this malfunction was probably due to sediment trapped in the gauging pipe or a mechanical problem with the float. As a result, the event volume is significantly overestimated, to a level much larger than the volume recorded upstream in a river that does not have additional tributaries between stations. Where possible, erroneous data such as these were corrected and data quality was improved.

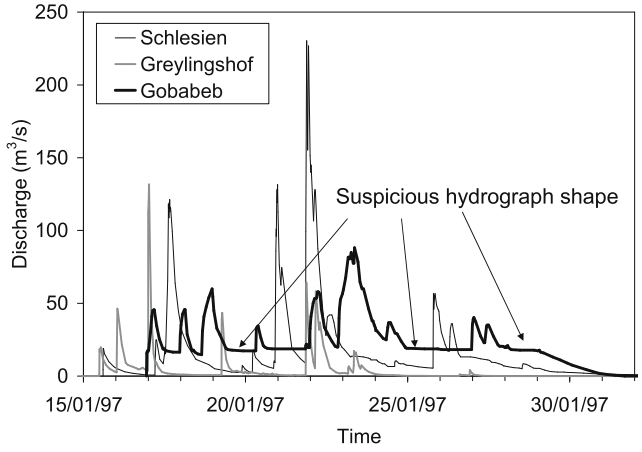

Fig. 3. An example of faulty data at the Gobabeb station (thick black line) for the flood event of January 1997. The hydrograph remains at a constant high discharge level rather than showing a typical desert recession to near zero. This most probably reflects a malfunction at the station due to sediment trapped in the gauging pipe or a mechanical problem with the float. The hydrographs at the upstream stations (Schlesien, thin black line, and Greylingshof, thick gray line) appear to be correct.

Table 2 summarizes the quality of existing flood records (1960–2005) after corrections, for the three hydrometric stations along the Kuiseb River. In general, the records of the Schlesien and Greylingshof stations are better than those of the Gobabeb station. The flood-routing modeling effort below requires calibration and the use of high-quality data from the three stations for floods that have reached the downstream station. Four hydrological years with data meeting these requirements were selected for calibration (Table 2).

Flood-routing model

Model description

The flood-routing model is a numerical solution of the kinematic wave equations in which infiltration during channel flow (i.e., transmission loss) is considered. The kinematic wave model is most often applied for routing computation (Bras, 1990) and is a simplification of the full one-dimensional St. Venant equations that combine continuity and momentum–conservation equations. Although the kinematic wave model is a common choice for routing computation, including models for dry regions that consider transmission losses such as the KINEROS model (Smith et al., 1995), reservations have been reported concerning the applicability of this approximation for transmission-loss studies (Mudd, 2006). The comparison of the kinematic and diffusive wave models for the current analysis suggests that the latter option introduces larger numerical errors while not improving model performance given the uncertainties in the data (see Fig. 4 for simulations by the two models and the observed flow). The kinematic wave model was therefore selected as the routing model.

The model is described by the following two equations:

$$\frac{\partial A}{\partial t} + \frac{\partial Q}{\partial x} = q - wcf \tag{1}$$

$$Q = \alpha A^m \tag{2}$$

where t is time (s), x is length along the channel axis (m), Q is flow discharge (m^3/s), A is the wetted cross-sectional area (m^2), q is lateral inflow (m^2/s), w is the wetted width (m), $c = 3.6 \times 10^{-6}$ is a unit transformation coefficient, f is infiltration (mm/h), $m = 5/3$, and $\alpha = \sqrt{\frac{s}{nP^{2/3}}}$ where s is the channel-bed slope, n is Manning's roughness coefficient and P is the wetted perimeter (m). In the lower Kuiseb River (from the foothills of the Great Escarpment), the only

Table 2
Quality of existing flood record after corrections for the three hydrometric stations along the Kuiseb River from 1960 to 2005.

Year	Sc	Gr	Gob	Remarks/problems	Year	Sc	Gr	Gob	Remarks/problems
1960	g	–	–		1983	g	g	g	
1961	n	–	–		1984	g	g	g	Calibration data
1962	g	–	–	Extreme flood	1985	g	g	g	
1963	n	–	–		1986	g	g	s	
1964	p	–	–	Two floods ok, one wrong	1987	g	g	p	
1965	p	–	–	Four floods ok, one wrong	1988	g	g	s	
1966	g	–	–		1989	g	g	p	
1967	g	–	–		1990	p	g	p	
1968	g	–	–		1991	p	p	p	
1969	g	–	–		1992	g	g	p	
1970	g	–	–		1993	p	g	p	
1971	g	–	–		1994	g	g	g	Calibration data
1972	g	–	–		1995	g	g	p	
1973	g	–	–		1996	g	g	s	
1974	g	g	–		1997	g	g	n	
1975	g	g	–		1998	g	g	n	
1976	g	n	–		1999	p	p	g	Extreme flood
1977	g	g	g	Calibration data	2000	g	g	p	
1978	g	g	p		2001	g	g	n	
1979	g	g	n		2002	g	g	g	Calibration data
1980	g	g	n		2003	p	p	p	
1981	g	g	n		2004	n	n	n	
1982	g	g	n		2005	g	p	p	

Sc-Schlesien, Gr-Greylingshof, Gob-Gobabeb; 1960 = Hydrological year 1960/61; – = not operational (pre-measurement period). From 1977, all three stations were operational. Data quality indicators: g = good; s = sufficient; p = part (but not all) of the data of sufficient quality; n = no floods reached this station during the hydrological year; and Calibration data = data used for model calibration.

significant source of water flow is from upstream tributaries in the more rainy headwaters, and lateral flow from local hillslopes is therefore assumed to equal zero.

Combining Eqs. (1) and (2) above and applying an explicit numerical scheme (Bras, 1990) resulted in the finite-differences equation:

$$A_{i+1}^{j+1} = A_{i+1}^{j} - \alpha_{i+1}^{j}\Delta t\left[\frac{(A_{i+1}^{j})^m - (A_i^j)^m}{\Delta x}\right] - w_{i+1}^{j} cf_{i+1}^{j+1}\Delta t \qquad (3)$$

where index i represents the length domain along the channel with grid points separated by a distance Δx, and index j represents the time domain with grid points separated by intervals of Δt .

For each channel segment, Δx is defined as the segment length (Table 1, column 5) divided by 50 (400–1100 m for the different segments) and Δt is defined as $\Delta x/10$ (40–110 s). These intervals are selected to provide negligible numerical errors and to prevent numerical instability. Initial dry conditions are assumed for the arid river and upstream flow as boundary conditions, which provide values for A_i^1 and A_1^j for all i and j.

The explicit scheme in Eq. (3) is then applied to solve A overall grid points. The wetted width, w, and the parameter α may change during the flow as a function of wetted area.

The infiltration process into the alluvial channel-bed is represented in the model according to Dahan et al. (2008) experimental results from the Kuiseb River, indicating a constant infiltration rate in general and zero infiltration when groundwater level reaches the surface. Accordingly, a constant infiltration rate is assumed in the model conditioned on groundwater level lower than surface level. The potential infiltrated volume at each Δt time step and each Δx channel length unit is the constant infiltration rate multiplied by the wetted width of the channel: *wcf*. The actual infiltration volume per unit width is limited by the wetted cross-sectional area, A_{i+1}^{j+1},computed initially without the infiltration component. Note that the wetted width may change during flow according to the water level in the cross-section.

Change in the alluvial aquifer groundwater level in response to the infiltrated flood water is estimated with a simplified model component based on the following assumptions: (1) all of the infiltrating water reaches the aquifer and is spread uniformly over its area; (2) the groundwater level decays at a constant rate representing the processes of evapotranspiration and consumption by pumping; and (3) when groundwater level reaches the surface, infiltration stops (Dahan et al., 2008). It should be emphasized that the above model components are intended to roughly estimate the general trends in groundwater levels resulting from flood water recharge over the 46-year record. Exact computation of groundwater flow requires more sophisticated groundwater models and is beyond the scope of the current study.

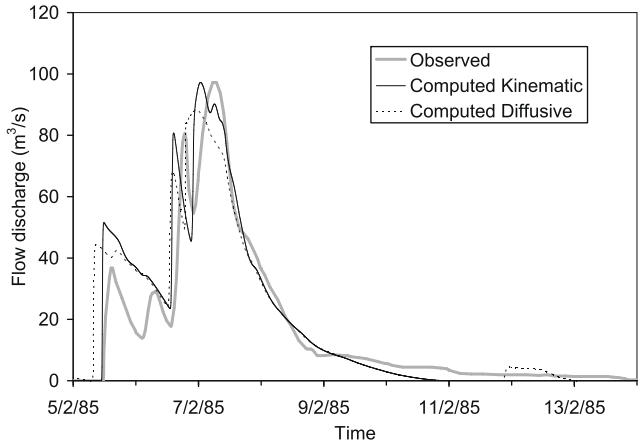

Fig. 4. A comparison of flood hydrographs computed by the kinematic wave model (thin solid line), the diffusive wave model (thin dashed line) and the observed hydrograph (thick gray line) at the Gobabeb hydrometric station for the flood of February 1985.

Model application to the lower Kuiseb River

The routing model was applied to the lower Kuiseb River between the upstream hydrometric stations of Schlesien and Grey-

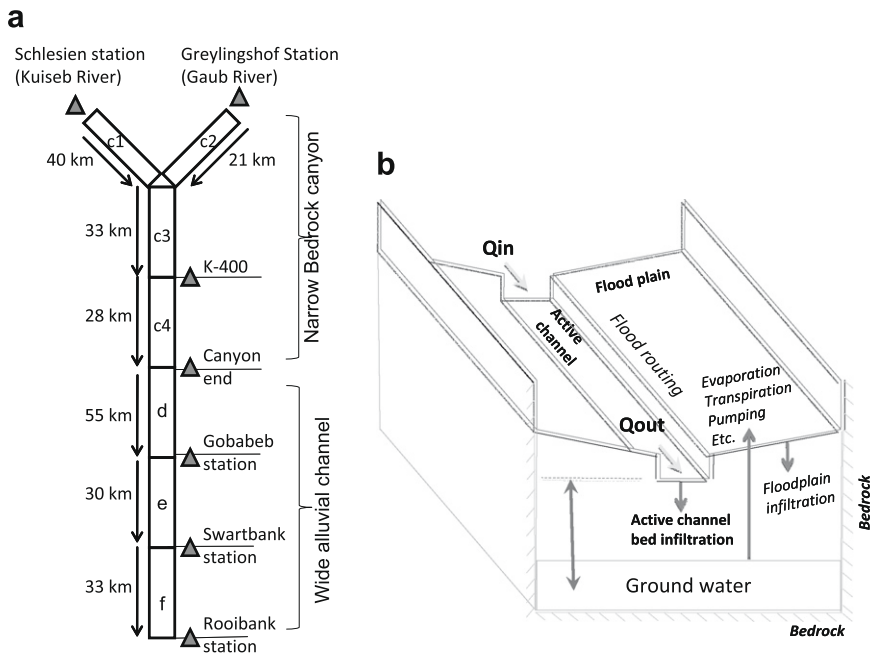

Fig. 5. (a) Model segments of the Kuiseb River (Table 1) and (b) schematic cross-section of the alluvial river (downstream of the canyon end) and the main processes computed by the model.

lingshof and the downstream Rooibank station (Fig. 1b, Table 1). The division into model segments is more or less similar to the earlier-described geographical segmentation ('The Kuiseb River', Fig. 1b and Table 1), except that some segments are split to include computation for points of interest (Fig. 5a, Table 1). The modeled part lies from segment c to segment f. The canyon segment, c, is divided in the model into four sub-segments (Fig. 5a). The first two (c1, c2) are the Kuiseb and Gaub Rivers starting at the Schlesien and Greylingshof stations, respectively, and ending at the joining of the two rivers. The next two (c3, c4) represent the Kuiseb River Canyon, which is divided at a point of interest (termed K-400) in which paleoflood observations were conducted but not included in the current analysis (Grodek et al., 2007). The next three model segments follow segments d–f in 'The Kuiseb River' and Fig. 1b.

For each segment, model parameters related to the river cross-section and groundwater were determined. Table 3 lists the sources of information or methodology used to set each model parameter and the values of most of the parameters for each segment are listed in Table 1. Manning's roughness coefficient was assumed uniform for all segments and was determined by calibration. For the upstream four segments up to the canyon end (c1–c4; Fig. 1b), zero infiltration was assumed according to observations of limited water loss along the canyon (see 'The Kuiseb River', segment c). For the lowest three segments (d–f; Fig. 1b), a uniform constant infiltration rate parameter was assumed and determined by calibration. The same value of infiltration rate was also assumed for the floodplains: although we realize that this point is questionable, no other data were available. It will be shown below, however, that the total infiltrated volume is relatively insensitive to this floodplain parameter.

Table 3
Parameters used in the routing model.

Parameter	Obtained by
Channel parameters	
Channel section slope, S	Field and GIS
Channel section length	Field and GIS
Manning roughness coefficient, n	Calibration (uniform for all segments)
Infiltration rate, f	Assumed zero for the upper four segments and found by calibration for the lower three
Cross-section parameters	
Active width	Aerial photographs and algorithm (see Model application to the lower Kuiseb River)
Section wall height and slope	Field and aerial photographs
Full section width	Field and aerial photographs
Subsurface parameters	
Aquifer width	Borehole cross-sections
Porosity	Lab
Minimal groundwater level	Long-term data
Groundwater level decay rate between events	Estimated from well data

A rectangular cross-section was assumed for the upstream segments all the way to the canyon's end (c1, c2, c3, and c4). In the three segments downstream of the canyon (d–f), the floodplains are represented as sloping planes in the model cross-section (Fig. 5b). The height of the channel cross-section from the thalweg of the active channel to the floodplain and the slope of the floodplains were measured in the field at several sites, and a characteristic cross-sectional valley geometry was determined. The width of the active channel varies along the channel.

The average active channel width was determined by applying a GIS algorithm developed specifically for this purpose. From 2-m pixel resolution aerial photographs, the 220-km channel path from the Schlesien and Greylingshof stations to the Rooibank station was digitized. The digitized lines represent the active channel and the floodplains. The lines were discretized into 1-m intervals and the distance between each pair of points on both sides of the active channel and the floodplain was calculated. This procedure produced more than 200,000 width data points along the entire channel. For each of the seven model segments described above, the average values of the active channel width and floodplain width were computed.

The other parameters used in the model are related to groundwater level computation and are relevant to the lowest three segments where channel infiltration occurs (Table 1). The parameters

required for the transformation of infiltration rate into groundwater level according to the assumptions listed in 'Model description' are: aquifer length, aquifer width, aquifer porosity, and constant decay rate of groundwater level. Aquifer length is taken as the length of the channel segment. Aquifer width is estimated from cross-sections of boreholes and exposed bedrock at the sides of the valley. For segment d (Fig. 1b, Table 1), where the aquifer is only a few meters below the surface, an intermediate value of 100 m lying between the actual aquifer width (~200 m) and the active channel width (~50 m) was used in the analysis. The effect of this selection on downstream flow was small, as confirmed by sensitivity analyses (not shown). A porosity of 0.4 was estimated as the representative value based on laboratory and in situ field measurements (Dahan et al., 2008). The groundwater level recession rate, representing the total effect of evapotranspiration and pumping, was determined based on well data in the lowest two segments for years without floods (i.e., no recharge). A lower threshold of groundwater level was estimated from well data and from 3 years of groundwater level measurements near Gobabeb by Dahan et al. (2008) and others. The starting level in the first year of simulation was given an arbitrary value because no information exists on this value.

Model calibration and validation

Model calibration

The calibration process was based on the four hydrological years (Table 2) that presented good-quality data from Schlesien, Greylingshof, and Gobabeb. The upstream flow served as input, and observed and computed hydrographs at the Gobabeb station were compared. Two unknown model parameters, Manning's roughness coefficient, n, and infiltration rate, f, were determined by calibration.

The flow parameters examined were: peak discharge, flow volume, infiltration volume, time of peak, and flow duration. These parameters were compared using two statistical functions—root mean square deviation (RMSD) and the Bias estimator:

$$\mathrm{RMSD} = \sqrt{\frac{1}{n}\sum_{i=1}^{n}(C_i - O_i)^2}, \text{ and} \tag{4}$$

$$\mathrm{Bias} = \frac{1}{n}\sum_{i=1}^{n} C_i - \frac{1}{n}\sum_{i=1}^{n} O_i \tag{5}$$

where C_i is the computed parameter value for event i, O_i is the observed parameter value for event i, and n is the number of events. The optimization procedure searches for the parameter values that minimize the RMSD function and the absolute value of the Bias function. The search is done by equal-interval jumps over the parameter space, with Manning's coefficient examined in the range of 0.01–0.07 with intervals of 0.005 and the infiltration rate in the range of 0–15 mm/h with intervals of 0.5 mm/h.

The five compared flow parameters and the two functions provided 10 objective functions for each combination of parameter values examined. The response surfaces of each of these objective functions were examined to study their sensitivity (Fig. 6). The RMSD objective functions of the infiltration volume, flow volume and duration were mainly sensitive to the infiltration rate parameter (Fig. 6a, b and, e), while the RMSD objective functions of the peak discharge and time of peak (Fig. 6c and d) were mainly sensitive to Manning's roughness coefficient. A small correlation between the two calibrated parameters was indicated by the diagonal trend of the contours in the response surfaces. The response surfaces of the five Bias objective functions showed similar behavior.

The identification of an optimal parameter set is not as straightforward as when calibrating a single objective function. Clearly, there is no one parameter set that provides a best match for all

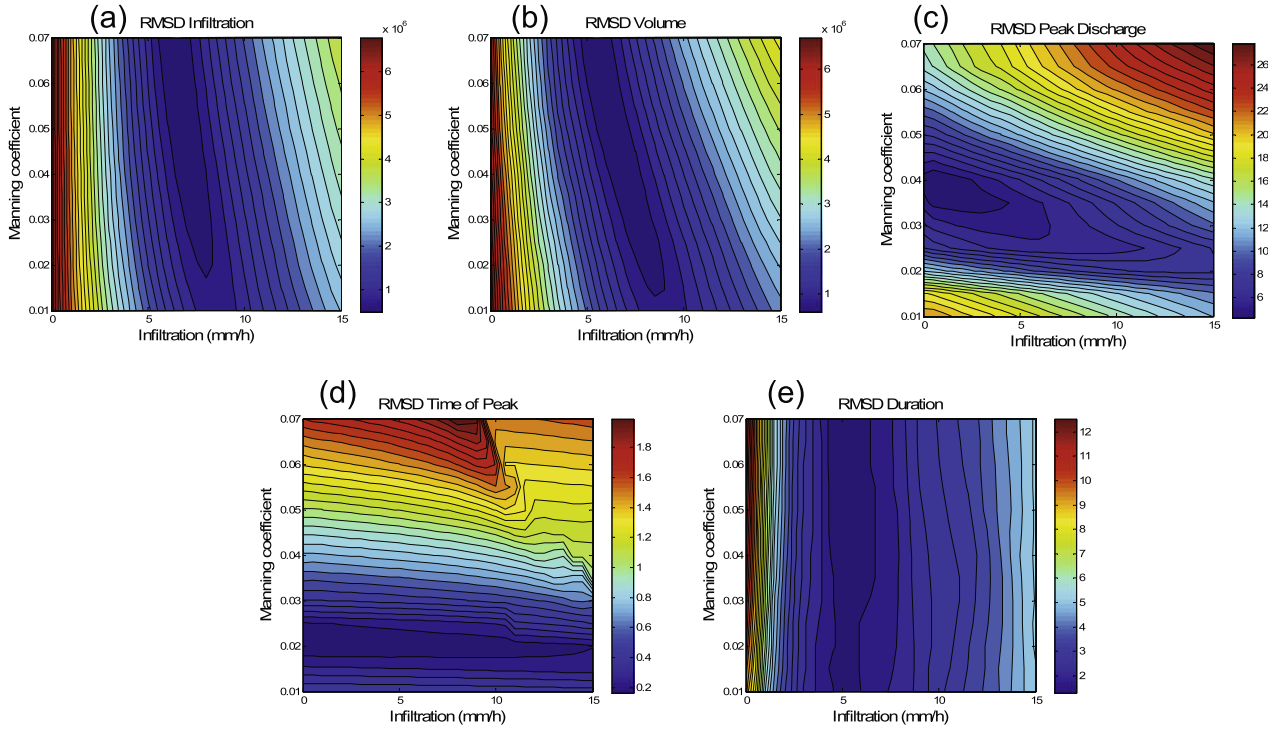

Fig. 6. Response surfaces of the Root Mean Square Difference (RMSD) function for the infiltration (x-axis) and Manning's roughness coefficient (y-axis) model parameters, computed for the flow parameters: (a) infiltration volume, (b) flow volume, (c) peak flow discharge, (d) time of flow peak, and (e) flow duration. Each pixel represents the RMSD value of observed and computed floods for the calibration data set.

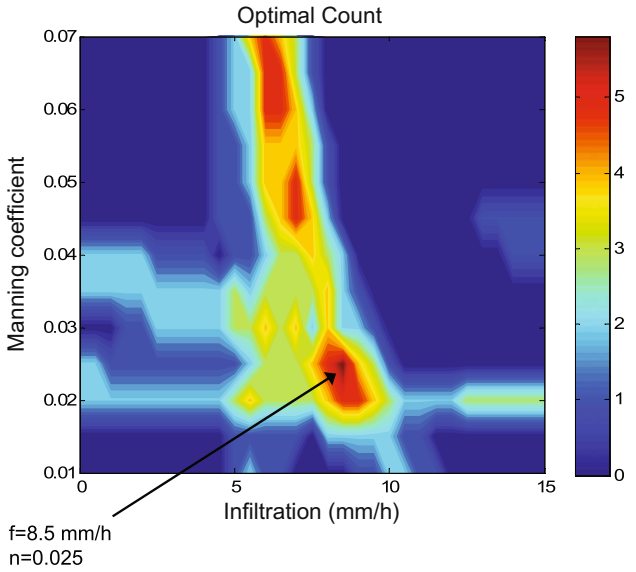

Fig. 7. For each combination of calibrated parameters, the number of objective functions (out of 10) in which the parameter set was in the lowest (i.e., best) 10th percentile. The dark red color indicates parameters that are best according to the largest number of objective functions and are therefore selected as optimal parameters. The arrow points to the selected parameter set.

10 cases; rather, we are looking for a tradeoff solution in this multi-objective optimization problem. The approach taken here is to derive an optimal zone for each of the 10 scores and to select the parameter set that is contained within the largest number of such zones. An optimal zone was defined here as the zone in the parameter space with objective function values that are in the lowest (i.e., best) 10th percentile. Fig. 7 presents the resultant response surface where, for each combination of the two calibration parameters, the number of optimal zones containing that combination (between zero and 10) is shown. The combination with the highest number is selected. The optimal parameter set found was $f = 8.5$ mm/h and $n = 0.025$, as its function value was in the optimal zone for six out of the 10 objective functions, more than any other parameter set examined (Fig. 7). It was close to, but not included in, the optimal zones of the RMSD and Bias functions of the duration and time of peak parameters. Thus while this set presents a maximal global value (Fig. 7), another local optimum can be approximately identified at around $f = 5$–10 mm/h and $n > 0.02$.

Fig. 8 presents a comparison of observed and computed values of peak discharge, flood volume and infiltration volume for the four calibration years. The other examined flow parameters indicated a similar level of fitness. It is important to emphasize that the constant infiltration rate identified by this modeling study, 8.5 mm/h, is in the range of the recharge fluxes of 7–15 mm/h reported for the Kuiseb River by Dahan et al. (2008), based on wetting-front propagation measured by TDR in the vadose zone.

Model validation

Model validation is a desirable step in the modeling process that helps evaluate the model with data not used for its calibration.

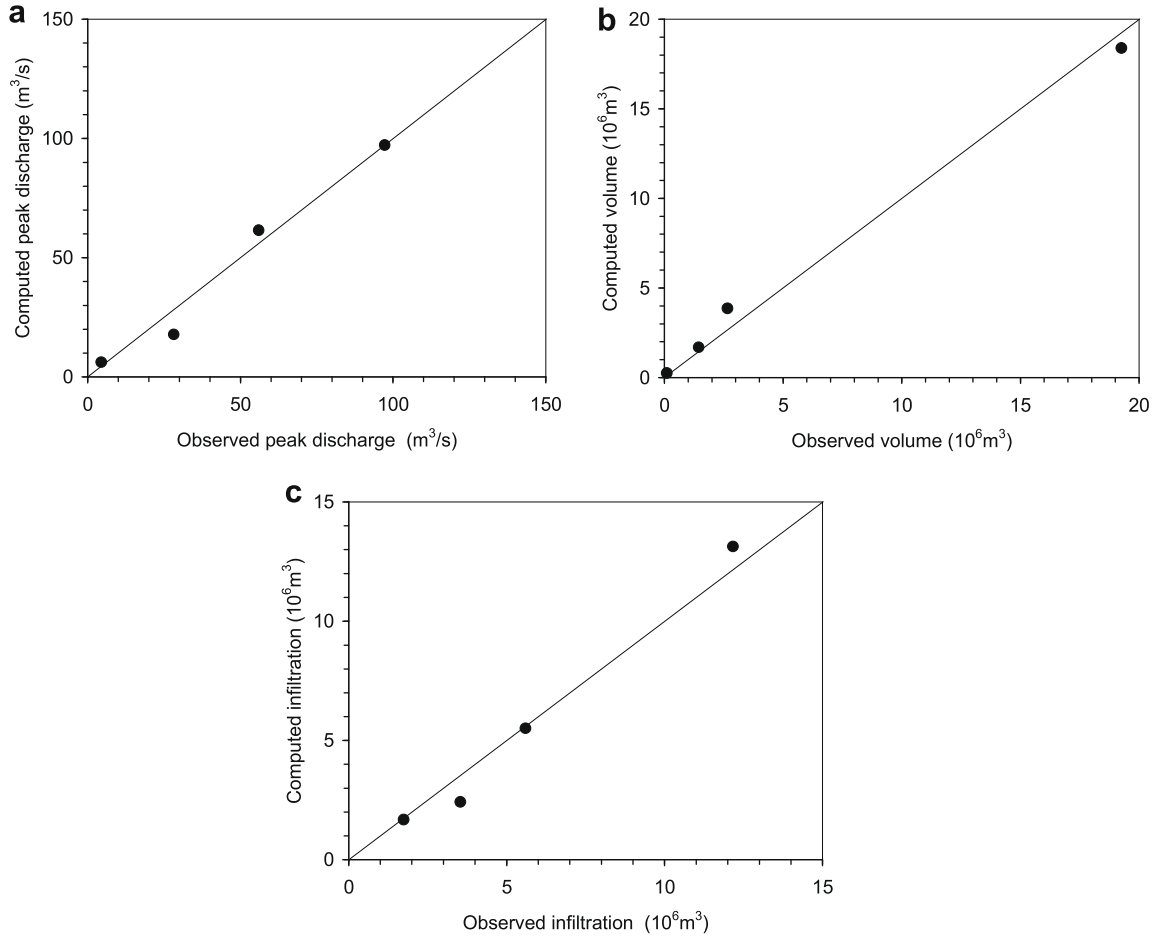

Fig. 8. Fit between observed and computed flood peak discharge (a), flood volume (b) infiltration volume, and (c) for the calibration data with the selected parameter set.

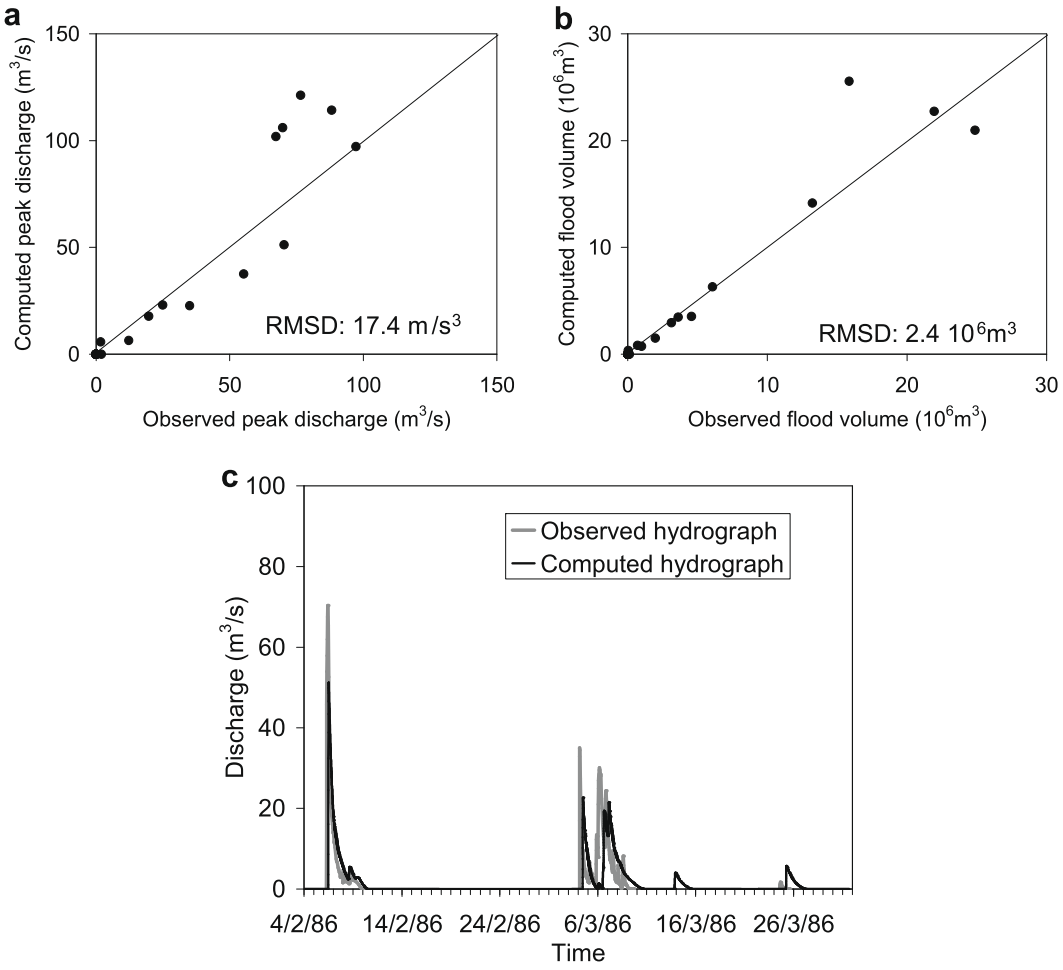

Fig. 9. Observed and computed peak discharge (a) and flood volume (b) for the validation flood events, and (c) a comparison of observed and computed flood hydrographs for the year 1985/1986 for the Gobabeb station.

Validation was done for data of good or sufficient quality that had not been used for calibration (Table 2). Fig. 9a and b presents the comparison of observed and computed peak discharge and volumes for the validation flood events at the Gobabeb station. The resultant RMSD of these data were 17.4 m^3/s and 2.4×10^6 m^3 for the peak discharge and flood volume, respectively. Comparison of observed and computed flood hydrographs for 1 year is also shown in Fig. 9c. The above results indicated a generally good fit and low error values for the validation flood cases.

Another test for the model's reliability was to examine the computed groundwater level data against observed water levels in wells along the river since the 1980s. Evidently, there was some variability of piezometric level over the studied reach and therefore, the averaged level in the observed wells was compared to the estimated groundwater levels (Fig. 10). Note that only the relative change in water level can be compared between the observed and computed data since the absolute water level in the first year of simulation is unknown. For the sake of visual comparison, the computed water level was shifted to match the level of the observed data. Fig. 10 indicates that the model is capable of simulating the two major groundwater level rises in 1997 and 2000, although it somewhat underestimates the latter. Also noticeable in the figure is a significant change between the groundwater levels of 1960–1980 and those of the following 20-year period. For the last segment (Rooibank), a slow decay is shown in the earlier period while a pronounced drop can be noted in the second period. The decay difference can be attributed to a decrease in flood frequency during the 1980s, with no floods reaching the most downstream reach for about 5 years (1980–1984).

Simulations and sensitivity analysis

Simulating Kuiseb River flow, transmission losses, and recharge

Flow, transmission loss and recharge records for the Kuiseb River were simulated for the years 1960–2005 with the upstream flow data from the Schlesien and Greylingshof stations, except in the case of the extreme flood of 1999, for which data were missing from the upstream records (Table 2). Therefore, the model was used to estimate an upstream hydrograph in Schlesien by iteration and by best-fitting the routing results to the available downstream hydrograph. In all other cases, the downstream hydrograph was simulated. For the period 1960–1977 when Schlesien was the only operating station, zero flow from the Gaub River was assumed. This assumption was made because the Schlesien station drains 6200 km^2 of wetter elevated areas (150–350 mm), while Greylingshof Station (Gaub River) drains 2900 km^2 at drier and lower elevations (150–250 mm) (Fig. 1b); as a result: (a) the volumes observed at Greylingshof are only 17% of the total volume and (b) flood peaks from the Gaub River reach the point of confluence with the Kuiseb River with a time shift of hours or days. By setting hydrographs of Greylingshof to zero, flood volumes and peaks computed for 1960–1977 are probably underestimated by about 15–20%.

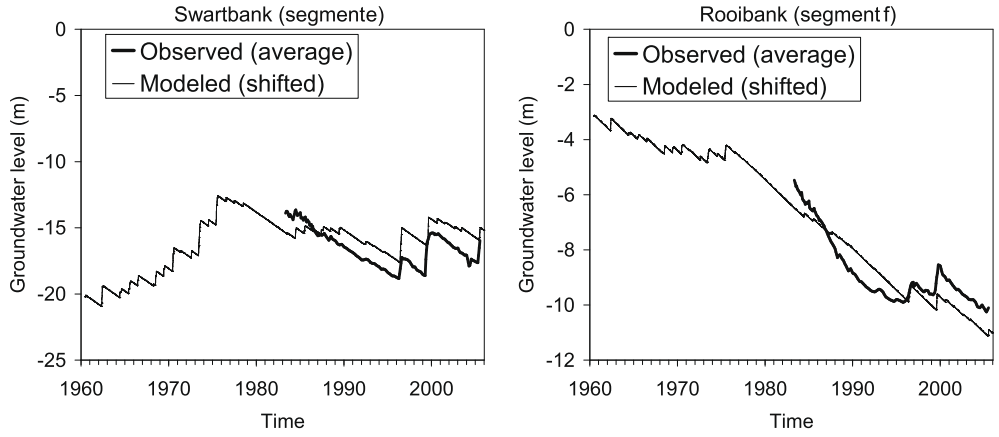

Fig. 10. Observed and modeled daily groundwater levels for the Swartbank segment (e) and Rooibank segment (f). Observed data are averages of well levels in each segment (available from the 1980s). Note that only the relative change in water level can be compared between the observed and modeled data since the absolute water level in the first year of the simulation is unknown, and the modeled data have been shifted to match the level of the observed data.

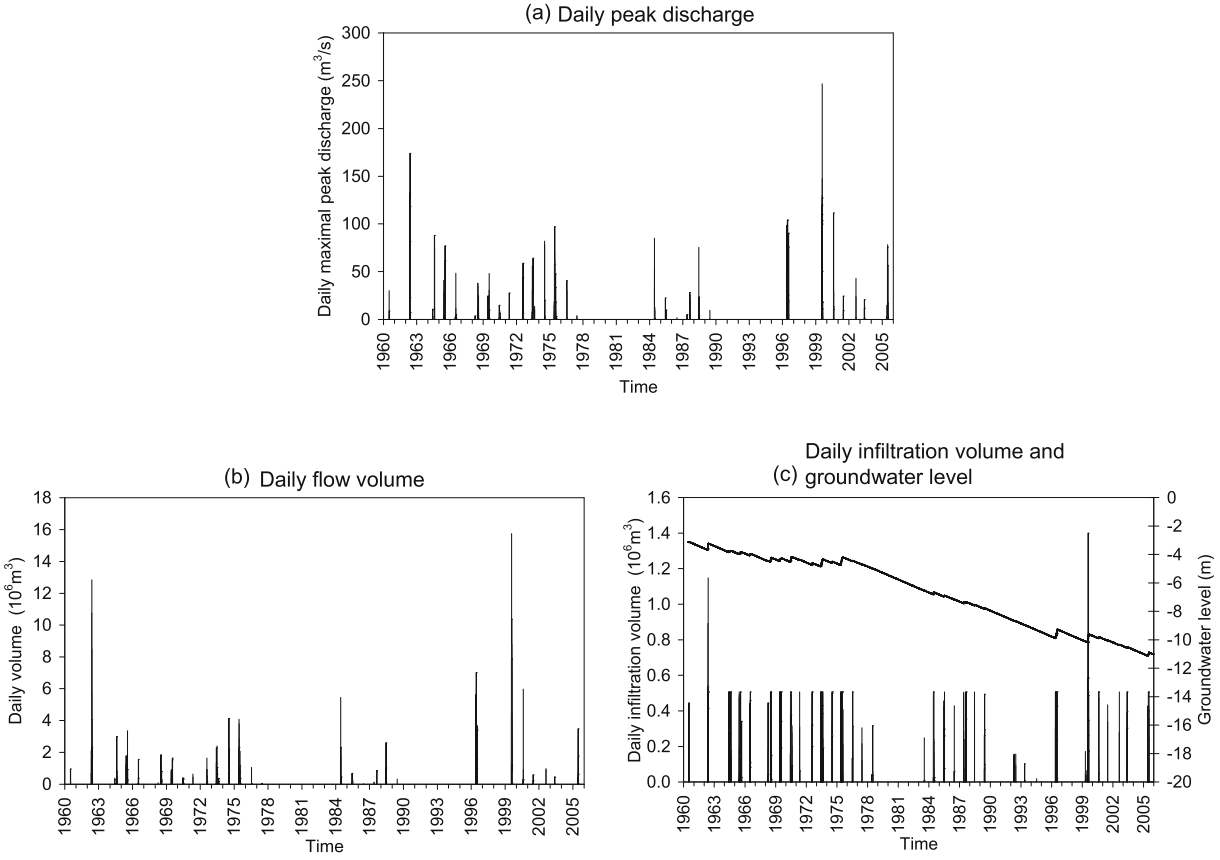

Fig. 11. Model simulation results for the Rooibank segment (f): (a) daily peak discharge, (b) daily volume, and (c) daily infiltration volume (bars) and groundwater level (line).

The main interest here was in the records for the Gobabeb, Swartbank and Rooibank river segments (segments d–f), where flood water is the main source of water for rural and urban communities along the river. Fig. 11 presents an example of modeled data for the Rooibank segment (segment f), showing daily data for flow peak discharge and volume at the downstream end of the segment, and infiltration volume and groundwater level for the entire segment length. The figure shows that for most of the flows, the daily infiltration volume is the same and it is strongly defined by the constant rate of infiltration (8.5 mm/h) through the entire active channel width and channel length throughout the day. Lower daily infiltration volumes result from flow that does not last for a full day or does not reach the downstream end. For two flood events (25 Jan 1963 and 29 Mar 2000), infiltration volumes (Fig. 11c) were higher than for all other events resulting from flow that exceeded the banks of the active channel and caused infiltration of water over the floodplains.

The 46-year simulation included 115 flood events. Table 4 provides the statistics of the characteristics in each segment of the simulated floods. These results indicate a respective 66% and 64%

Table 4
Summary statistics of floods in the river segments for the years 1960–2005.

Segment	N	Annual volume (10^6 m^3)		Annual peak discharge (m^3/s)		Annual infiltration volume (10^6 m^3)	
		Average	Std	Average	Std	Average	Std
Schlesien and Greylingshof junction (c1, c2)	115	19.7	29.0	139.0	160.9	0.0	0.0
K-400 (c3)	115	19.7	29.0	113.9	139.6	0.0	0.0
Canyon end (c4)	115	19.7	29.0	99.0	126.3	0.0	0.0
Gobabeb (d)	70	12.8	22.9	61.0	79.5	6.6	5.9
Swartbank (e)	58	9.4	19.1	49.8	66.5	3.4	4.5
Rooibank (f)	45	6.7	15.8	37.9	51.3	2.7	3.9

N = number of floods available for the 46-years record.

reduction in flood volume and peak discharge over the 118-km length from the canyon's end to Rooibank (segments d–f) throughout the entire record. Less than 40% of the floods that exit the canyon reach all the way downstream to Rooibank. The overall transmission-loss rates along segments d–f of the sandy alluvial channel are nearly 570, 860, and, 990 m^3/km h, respectively. This rate increment is mainly the result of widening of the active channel downstream, a hypothesis that is supported by previous observations of constant infiltration rate under variable flood conditions and control of total recharge by active channel width and flood duration (Dahan et al., 2008).

Effect of flood and river characteristics on recharge to alluvial aquifer

Infiltration rate, flood peak discharge, and flood duration

Sensitivity analysis was applied to study the effects of flood and river characteristics on the Kuiseb River recharge. For future paleohydrology data interpretations, we examined the K-400 (Fig. 1b) routed peak discharges against infiltration volumes in the Rooibank segment (Fig. 12a). The result reveal a relatively low correlation (R^2 = 0.46) for peak discharge values >15 m^3/s, set as the threshold for having any recharge downstream, and a higher correlation (R^2 = 0.58) for the entire data set. Flow duration, on the other

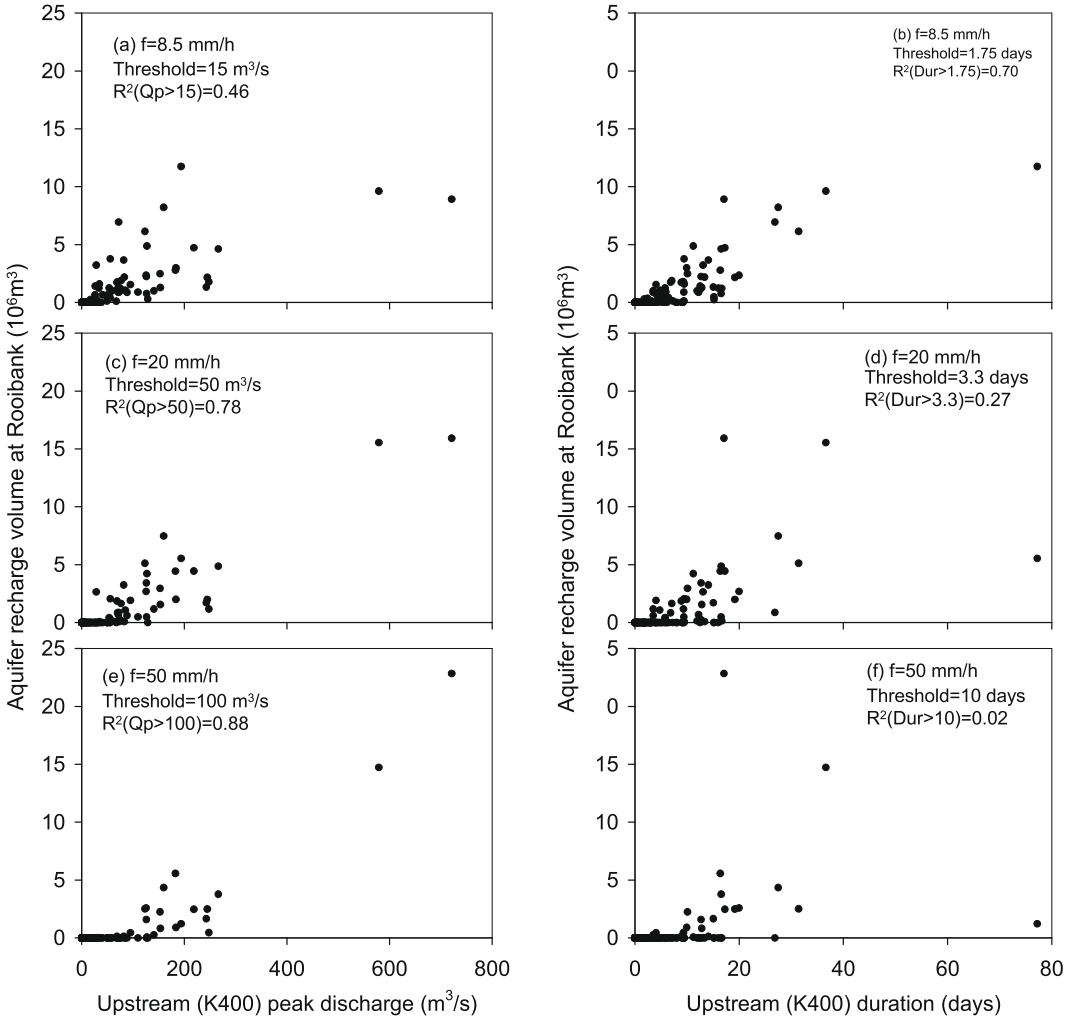

Fig. 12. Correlations between infiltration volumes in the Rooibank segment and upstream peak discharge (a, c, and e) or flow duration (b, d, and f) at the K-400 point (outlet point of segment c3, see Fig. 1) for infiltration rates of: 8.5 mm/h (a, b), 20 mm/h (c, d), and 50 mm/h (e, f).

hand, plays a more important role (R^2 = 0.70; Fig. 12b), as confirmed by the direct infiltration measurements in Gobabeb (Dahan et al., 2008). Although the relationships are not necessarily linear in this plot, the linear correlation value is consistent and comparable with the other relations examined here.

Fig. 12c–f show the relations between modeled peak discharge and flow duration at the upstream reach (K-400) and the estimated infiltration volume at Rooibank, assuming average infiltration rates of 20 and 50 mm/h, respectively. As infiltration increases, the limitation on infiltration volume per unit time becomes less pronounced, resulting in a clearer threshold and higher correlation of upstream peak discharges and downstream infiltration volumes. The opposite is observed for the relations between upstream flow duration and infiltration volume; the correlation decreases with an increase in infiltration rate.

Floodplain infiltration

The effect of floodplain infiltration was examined by comparing the modeled water volume infiltrating the Rooibank river segment once with the calibrated infiltration rate (8.5 mm/h) over the floodplain and once with the assumption of no infiltration over the floodplain. Using the latter assumption caused an increase of only 3% in the infiltrated volume in the Rooibank segment. Reduced infiltration rates over the floodplains was suggested by Dahan et al. (2008), with observed overbank deposits of alternating thin layers of sand and silt-clay.

The sensitivity of the Rooibank infiltration volume to the height of the floodplain above the active channel was also examined. Reducing the original value of 1.2 m found from field measurements (Table 1) to 0.8 m increased the Rooibank infiltration volume by 4%, and increasing the floodplain height to 1.6 m reduced the infiltration volume by 1%.

In these two described examinations, most of the volume change occurs for the two large events mentioned in 'Simulating Kuiseb River flow, transmission losses, and recharge'. The small effect of floodplain infiltration shown here indicates a relatively insignificant process when considering the river recharge system and the available flood magnitudes.

Large vs. small flood magnitudes

The question of which flood magnitudes contribute most to recharge was examined by comparing percentiles of upstream peak discharge with percentiles of downstream infiltration volume. The computation was done by assigning each flood the percentile of its upstream peak discharge (at the K-400 point, outlet of segment c3) and the percentile of its downstream infiltration volume (at Rooibank, segment f). The peak discharge percentiles of the floods that are in the upper 70% of the infiltration volume are presented in Fig. 13. The leftmost column shows this analysis with the original channel characteristics and infiltration rate. It indicates that 70% of the Rooibank infiltration volume is contributed by floods in the $\geqslant$63rd percentile in terms of upstream peak discharge. This means that because infiltration rates in the Kuiseb River are relatively low, both medium and large floods contribute to downstream recharge. As simulated infiltration rate increases, the large floods become more important and, in the simulation based on an infiltration rate of 50 mm/h, 70% of the infiltration volume at Rooibank would have been contributed by the highest floods, with percentiles of 93% and more.

At high infiltration rates, the small and medium floods do not generally reach the downstream parts of the arid alluvial river. While out of the 115 floods observed upstream, 46 reach the Rooibank segment when infiltration rate is 8.5 mm/h (Table 4), only 12 large floods flow all the way downstream, according to simulations with a 50 mm/h infiltration rate. As expected, the same effects are obtained by increasing channel length or cross-sectional width (four right columns in Fig. 13).

Discussion

Floods are a vital source of water in arid regions. This scarce water resource is mostly exploited from the local or regional alluvial aquifers which are recharged by flood water infiltrating along alluvial ephemeral river beds. This paper studies flood water infiltration (transmission losses) in the arid Kuiseb River of Namibia. People living along the river's desert route use the flood-recharged aquifer intensively and the area's entire ecology, particularly the riparian environment, depend on its water storage.

The main tool used in this study was a flood-routing model which was applied to a flood record covering 46 years after extensive quality checks and corrections. The model allows flow and recharge simulation, data reconstruction for missing records, and an investigation of relationships between flood, river and recharge characteristics. The numerical model was based on the kinematic wave model with an infiltration component and a relatively simple

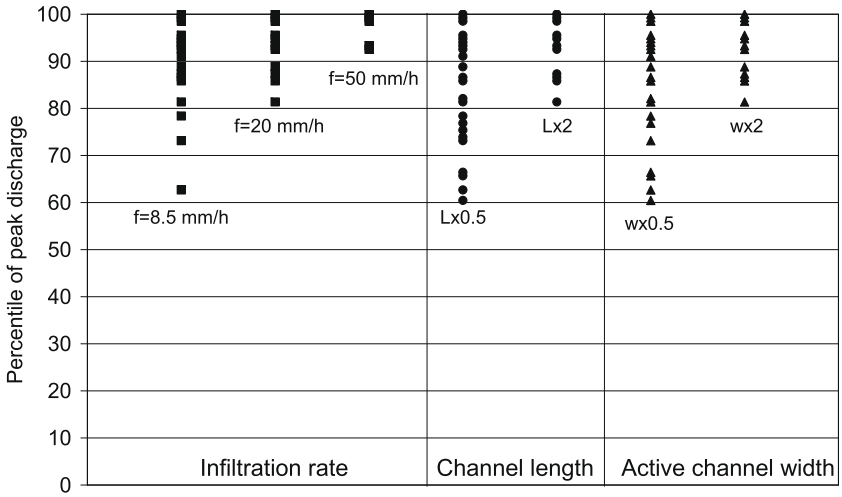

Fig. 13. Percentiles of peak flood discharge at upstream point K-400 (outlet of segment c3 in Fig. 1) that contribute a significant part of the downstream (Rooibank, segment f in Fig. 1) infiltration volume. The leftmost column shows this analysis with the original channel characteristics and infiltration rate. The second and third columns show the effect of using the infiltration rates of 20 and 50 mm/h, respectively. The fourth and fifth columns show the effect of multiplying the channel length by 0.5 and 2, respectively. The sixth and seventh columns show the effect of multiplying the active channel width by 0.5 and 2, respectively.

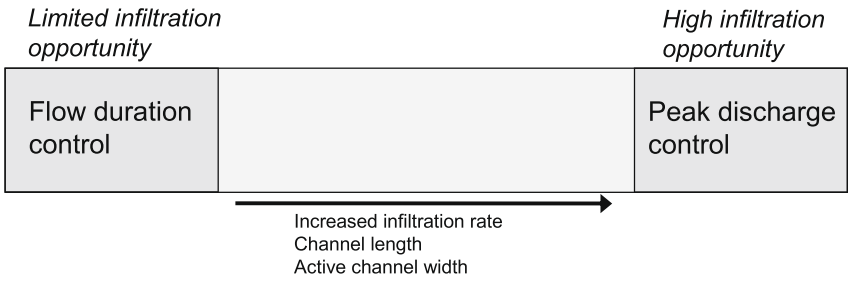

Fig. 14. Scheme presenting the importance of flood duration and peak discharge on infiltration volume for different channel characteristics. When channels are characterized by limited infiltration opportunities because they are short, narrow or have low infiltration rates, the infiltration process is more limited and the main control is flood duration. On the other hand, for channels that are long, wide, or have high infiltration rates, the opportunity for infiltration is higher and the flood magnitude (i.e., peak discharge) plays a more important role in determining infiltration volumes.

representation of the groundwater recharge process. It was shown that after calibration, the model was capable of simulating downstream flood hydrographs and changes in alluvial aquifer water levels with reasonable accuracy.

A major control of recharge is the infiltration rate of the channel-bed. Here, this parameter was determined by calibration, and was found to be 8.5 mm/h. An independent study in the same location (Dahan et al., 2008) found similar values based on soil-moisture measurements in the vadose zone. A comparison to infiltration rates reported in other studies revealed this value to be relatively low. For example, Shamir et al. (2007) applied a constant infiltration rate of 25 mm/h (based on Erwin, 2007) and Blasch et al. (2006) derived steady-state infiltration values in the range of 20–85 mm/h, both studies for rivers in southern Arizona. In the Negev desert in Israel, Lange et al. (1999) used infiltration rates between 40 and up to 400 mm/h and Osterkamp et al. (1995) applied values of 46–285 mm/h for a river in Abu-Dahbi. A similar observation of higher infiltration values, ranging from 10 to 60 mm/h, was found by the authors of this paper in a study on the Buffels River, South Africa (Benito et al., 2007). The reason for the relatively low infiltration rate in the Kuiseb River is probably related to the texture of the river-bed material, which is composed of fine sand with a high percentage of mica particles, whereas, for instance, on the Buffels River, the vadose zone is dominated by medium to coarse sand. Dahan et al. (2008) suggested that fine-grained texture lamina in the sandy alluvial sediments of the vadose zone regulate the infiltration fluxes and cause a relatively constant infiltration rate which is not very sensitive to changes in flood stage.

We argue that due to the limited infiltration rate, flow duration becomes an important factor in determining infiltration (and potentially recharge) volumes. We show that if infiltration rate is increased, the effect of flood duration becomes less important and at the same time, infiltration volume becomes more dependent on the magnitude of the flow. This result is in agreement with Parissopoulos and Wheater (1991) who showed a larger effect of flood duration on infiltrated volume for fine soil compared to sand.

The limited infiltration rate also plays a role in determining the relative long-term, cumulative importance of small, medium or large events on recharge. In general, due to transmission loss, not all upstream floods reach the downstream segments: high-magnitude floods have a better chance of doing so, and recharging the alluvial aquifer. In other words, the transmission loss acts as a low-pass filter on flood magnitude. If infiltration rate is not very high, the filtering effect will be less pronounced, as seen in the current study where both medium and large floods were found to be important. It is expected that with higher infiltration rates, the relative importance of high-magnitude floods will rise.

Lange (2005) suggested that mainly high-magnitude floods are significant for recharge in the Kuiseb River because their relatively high flow stages reach the overbank where width is significantly larger. The current study, however, shows that medium floods contribute significant recharge volume and the effect of infiltration from floodplain areas to the total infiltrated volume is small. Our study concludes that overbank infiltration from floods is not significant for aquifer recharge along the Kuiseb River, and this may be the case with other dryland rivers, especially when floodplain textures are made up of alternating sand and clay layers, as in the Kuiseb.

Fig. 14 summarizes the qualitative relations between the parameters examined in this study in terms of channel characteristics (infiltration rate, channel length, and channel width) and flow characteristics (flow duration, and peak discharge and infiltration into the alluvial channel). As one of the channel-limiting factors becomes less pronounced, the role of large-magnitude floods with respect to infiltration and recharge increases.

Conclusions

Flood routing and transmission losses in the lower reaches of the Kuiseb River are investigated in this study, focusing on: (1) quality control of the records; (2) modeling routing and transmission losses, and (3) studying the relationships between flood characteristics, river characteristics and recharge into the aquifers. The main conclusions inferred from the study are:

(1) he flow observations at upstream and downstream stations in the Kuiseb River of Namibia present a unique data set to study the processes of flood routing and alluvial aquifer recharge in arid to hyperarid rivers.
(2) Quality control of the data is a crucial step in the analysis.
(3) The kinematic wave model with added simplified modules for recharge is capable of simulating, with reasonable accuracy, flood discharge along the river and recharge to the alluvial aquifer in the lower parts of the river when fed with upstream flow data.
(4) The infiltration rate into the alluvial channel-bed is estimated by calibration to be 8.5 mm/h.
(5) Most of the recharge volume to the alluvial aquifer is from floods of medium and large magnitude. In rivers with different conditions of higher infiltration opportunities (e.g., higher channel-bed infiltration rates, longer or wider channels), a larger proportion of floods totally infiltrate on the way downstream. Consequently, under such conditions, recharge to the alluvial aquifer downstream is contributed mainly by large-magnitude floods.

Acknowledgements

The authors would like to thank the following organizations for providing the information necessary for this research: Namibia Water Corporation for groundwater measurement data; Ministry

of Agriculture, Water and Forestry, Department of Water Affairs, Hydrology Division, Windhoek, and Namibia for hydrological data. The study was funded by the 6th framework of the European Community through the project "Flood Water Recharge of Alluvial Aquifers in Dryland Environments", WADE Project (Contract No. GOCE-CT-2003-506680). In addition, this research was supported in part by Grant No. CDR C24-026 from the US-Israel Cooperative Development Research Program, Bureau for Economic Growth, Agriculture, and Trade, US Agency for International Development. Special thanks to the Desert Research Foundation of Namibia and to Gobabeb Training and Research Center for providing the necessary tools and support that allowed this project to succeed. The authors thank three anonymous reviewers for their valuable comments.

References

Bate, G.C., Walker, B.H., 1993. Water relations of the vegetation along the Kuiseb River, Namibia. Madoqua 18 (2), 85–91.

Benito, G., Thorndycraft, V., Rico, M.T., Sanchez-Moya, Y., Sopena, A., Botero, B., Perez-Gonzalez, A., Dahan, O., 2007. Palaeoflood Hydrology and Floodwater Recharge on the Buffels River (Namaqualand, South Africa). The XVII INQUA Congress Cairns, Australia.

Blasch, K., Ferré, T.P.A., Hoffmann, J., Pool, D., Bailey, M., Cordova, J., 2004. Processes controlling recharge beneath ephemeral streams in southern Arizona. In: Hogan, J.F., Phillips, F.M., Scanlon, B.R. (Eds.), Groundwater Recharge in a Desert Environment. The Southwestern United States, AGU, Washington, DC, pp. 69–76.

Blasch, K.W., Ferre, T.P.A., Hoffmann, J.P., Fleming, J.B., 2006. Relative contributions of transient and steady state infiltration during ephemeral streamflow. Water Resources Research 42 (8). doi:10.1029/2005WR004049.

Bras, R.L., 1990. Hydrology: An Introduction to Hydrologic Science. Addison-Wesley Publishing Company. 643 pp.

Buono, A., Lang, D.J., 1980. Aquifer Recharge from the 1969 and 1978 Floods in the Mojave River Basin, California.

Costelloe, J.F., Grayson, R.B., Argent, R.M., McMahon, T.A., 2003. Modelling the flow regime of an arid zone floodplain river, Diamantina River, Australia. Environmental Modelling & Software 18 (8–9), 693–703.

Dahan, O., Tatarsky, B., Enzel, Y., Kulls, C., Seely, M., Benito, G., 2008. Dynamics of flood water infiltration and ground water recharge in hyperarid desert. Ground Water 46 (3), 450–461. doi:10.1111/j.1745-6584.2007.00414.x.

Dubief, J., 1953. Ruissellement superficiel au Sahara. Colloquvium International C.N.R.S. 35, 303–314.

El-Hames, A.S., Richards, K.S., 1998. An integrated, physically based model for arid region flash flood prediction capable of simulating dynamic transmission loss. Hydrological Processes 12 (8), 1219–1232.

Enzel, Y., 1992. Flood frequency of the Mojave River and the formation of late Holocene playa lakes, southern California. The Holocene 2, 11–18.

Enzel, Y., Wells, S.G., 1997. Extracting Holocene paleohydrology and paleoclimatology information from modern extreme flood events: an example from southern California. Geomorphology 19 (3–4), 203–226.

Erwin, G., 2007. Groundwater Flow Model of the Santa Cruz Active Management Area Microbasins International Boundary to Nogales International Wastewater Treatment Plant Santa Cruz County. Arizona Department of Water Resources, Arizona.

Freyberg, D.L., Reeder, J.W., Franzini, J.B., Remson, I., 1980. Application of the Green-Ampt model to infiltration under time-dependent surface-water depths. Water Resources Research 16 (3), 517–528.

Grodek, T., Enzel, Y., Benito, G., Beukes, H., Porat, N., Jacoby, Y., Dahan, O., Van Langenhove, G. Seely, M., 2007. The largest floods along the canyons of the Kuiseb and Gaub Rivers. In: Namibia 4th International Palaeoflood Workshop, Crete, Greece.

Guzman, A.G., Wilson, L.G., Neuman, S.P., Osborn, M.D., 1989. Simulating effect of channel changes on stream infiltration. Journal of Hydraulic Engineering-ASCE 115 (12), 1631–1645.

Hughes, D.A., Sami, K., 1992. Transmission losses to alluvium and associated moisture dynamics in a semiarid ephemeral channel system in southern Africa. Hydrological Processes 6 (1), 45–53.

Izbicki, J.A., Radyk, J., Michel, R.L., 2002. Movement of water through the thick unsaturated zone underlying Oro Grande and Sheep Creek Washes in the western Mojave Desert, USA. Hydrogeology Journal 10 (3), 409–427.

Jacobson, P.J., Jacobson, K.M., Seely, M.K. (Eds.), 1995. Ephemeral Rivers and Their Catchments: Sustaining People and Development in Western Namibia. Desert Research Foundation of Namibia, Windhoek, p. 160.

Knighton, A.D., Nanson, G.C., 1994. Flow transmission along an arid zone anastomosing river, Cooper Creek, Australia. Hydrological Processes 8 (2), 137–154.

Lange, J., 2005. Dynamics of transmission losses in a large and stream channel. Journal of Hydrology 306 (1–4), 112–126.

Lange, J., Leibundgut, C., Greenbaum, N., Schick, A.P., 1999. A noncalibrated rainfall–runoff model for large, arid catchments. Water Resources Research 35 (7), 2161–2172.

Mabbutt, J.A., 1977. Desert Landforms. MIT Press, Cambridge, MA.

Mendelsohn, J., Jarvis, A., Roberts, C., Robertson, T., 2002. Atlas of Namibia. David Philip Publication, Cape Town.

Mudd, S.M., 2006. Investigation of the hydrodynamics of flash floods in ephemeral channels: scaling analysis and simulation using a shock-capturing flow model incorporating the effects of transmission losses. Journal of Hydrology 324 (1–4), 65–79.

Osterkamp, W.R., Lane, L.J., Menges, C.M., 1995. Techniques of groundwater recharge estimates in arid semiarid areas, with examples from Abu-Dhabi. Journal of Arid Environments 31 (3), 349–369.

Parissopoulos, G.A., Wheater, H.S., 1991. Effects of wadi flood hydrograph characteristics on infiltration. Journal of Hydrology 126 (3–4), 247–263.

Renard, K.G., Keppel, R.V., 1966. Hydrographs of ephemeral streams in the Southwest. Journal of the Hydraulics Division, Proceedings of the American Society of Civil Engineers 92, 33–52.

Schick, A.P., 1988. Hydrologic aspects of floods in extreme arid environments. In: Baker, V.R., Kochel, R.C., Patton, P.C. (Eds.), Flood Geomorphology. Wiley Interscience, New York, pp. 189–203.

Seely, M.K., Buskirk, W.H., Hamilton III, W.J., Dixon, J.E.W., 1981. Lower Kuiseb River perennial vegetation survey. Journal of the South West Africa Scientific Society 34 (35), 57–86.

Shamir, E., Meko, D.M., Graham, N.E., Georgakakos, K.P., 2007. Hydrologic model framework for water resources planning in the Santa Cruz River, southern Arizona. Journal of the American Water Resources Association 43 (5), 1155–1170.

Sharma, K.D., Murthy, J.S.R., 1994. Estimating transmission losses in an arid region. Journal of Arid Environments 26 (3), 209–219.

Shentsis, I., Meirovich, L., Ben-Zvi, A., Rosenthal, E., 1999. Assessment of transmission losses and groundwater recharge from runoff events in a wadi under shortage of data on lateral inflow, Negev, Israel. Hydrological Processes 13 (11), 1649–1663.

Smith, R.E., Goodrich, D.C., Woolhiser, D.A., Unkrich, C.A., 1995. KINEROS: a kinematic runoff and erosion model. In: Singh, V.P. (Ed.), Computer Models of Watershed Hydrology. Water Resources Publication, Highlands Ranch, pp. 697–732.

Sorman, A.U., Abdulrazzak, M.J., MorelSeytoux, H.J., 1997. Groundwater recharge estimation from ephemeral streams. case study: Wadi Tabalah, Saudi Arabia. Hydrological Processes 11 (12), 1607–1619.

Theron, G.K., Van Rooyen, N., Van Rooyen, M.W., 1980. Vegetation of the lower Kuiseb River. Madoqua 11 (4), 327–345.

Thornes, J.B., 1994. Catchment and channel hydrology. In: Abrahams, A.D., Parsons, A.J. (Eds.), Geomorphology of Desert Environments. Chapman & Hall, London, pp. 257–287.

Tooth, S., 2000. Process, form and change in dryland rivers: a review of recent research. Earth-Science Reviews 51 (1–4), 67–107.

Vanney, J.R., 1960. Pluie et crue dans le Sahara nord-occidental, vol. 4. Memoirs Regioneaux de l'Institute des Recherches Sahariens, Algiers.

Walters, M.O., 1990. Transmission losses in arid region. Journal of Hydraulic Engineering-ASCE 116 (1), 129–138.